

# Auditory sensitivity provided by self-tuned critical oscillations of hair cells

Sébastien Camalet\*, Thomas Duke\*<sup>†‡</sup>, Frank Jülicher\* and Jacques Prost\*

\*Institut Curie, PhysicoChimie Curie, UMR CNRS/IC 168,  
26 rue d'Ulm, 75248 Paris Cedex 05, France

<sup>†</sup>Niels Bohr Institute, Blegdamsvej 17, 2100 Copenhagen, Denmark

<sup>‡</sup>Cavendish Laboratory, Madingley Road, Cambridge CB3 0HE, UK

We introduce the concept of *self-tuned criticality* as a general mechanism for signal detection in sensory systems. In the case of hearing, we argue that active amplification of faint sounds is provided by a dynamical system which is maintained at the threshold of an oscillatory instability. This concept can account for the exquisite sensitivity of the auditory system and its wide dynamic range, as well as its capacity to respond selectively to different frequencies. A specific model of sound detection by the hair cells of the inner ear is discussed. We show that a collection of motor proteins within a hair bundle can generate oscillations at a frequency which depends on the elastic properties of the bundle. Simple variation of bundle geometry gives rise to hair cells with characteristic frequencies which span the range of audibility. Tension-gated transduction channels, which primarily serve to detect the motion of a hair bundle, also tune each cell by admitting ions which regulate the motor protein activity. By controlling the bundle's propensity to oscillate, this feedback automatically maintains the system in the operating regime where it is most sensitive to sinusoidal stimuli. The model explains how hair cells can detect sounds which carry less energy than the background noise.

Detecting the sounds of the outside world imposes stringent demands on the design of the inner ear, where the transduction of acoustic stimuli to electrical signals takes place [1]. The hair cells within the cochlea, which act as mechanosensors, must each be responsive to a particular frequency component of the auditory input. Moreover, these sensors need the utmost sensitivity, since the weakest audible sounds impart an energy, per cycle of oscillation, which is no greater than that of thermal noise [2]. At the same time, they must operate over a wide range of volumes, responding and adapting to intensities which vary by many orders of magnitude. Clearly, some form of non-linear amplification is necessary in sound detection. The familiar resonant gain of a passive elastic system is far from sufficient for the required demands, because of the heavy viscous damping at microscopic scales [3]. Instead, the cochlea has developed active amplification processes, whose precise nature remains to be discovered.

There is strong evidence that the cochlea contains force-generating dynamical systems which are capable of

executing oscillations of a characteristic frequency [4–10]. In general, such a system exhibits a Hopf bifurcation [11]: as the value of a control parameter is varied, the behavior abruptly changes from a quiescent state to self-sustained oscillations. When the system is in the immediate vicinity of the bifurcation, it can act as a nonlinear amplifier for sinusoidal stimuli close to the characteristic frequency. That such a phenomenon might occur in hearing was first proposed by Gold [3], more than 50 years ago. The idea was recently revived by Choe, Magnasco and Hudspeth [12], in the context of a specific model of the hair cell. No general analysis of the amplification afforded by a Hopf bifurcation has been provided, however, and no theory has been advanced to explain how proximity to the bifurcation point might be ensured.

In this paper, we provide both a generic framework which describes the known features of acoustic detection, and a detailed discussion of the specific elements which could be involved in this detection. We first derive the general resonance and amplification behavior of a dynamical system operating close to a Hopf bifurcation and emphasize that such a system is well-suited to the ear's needs. In order for active amplification to work reliably, tuning to the bifurcation point is crucial. We introduce the concept of a *self-tuned Hopf bifurcation* which permits the favorable amplification properties of a dynamical instability to be obtained in a robust way. Self-tuning maintains the system in the proximity of the critical point and is achieved by an appropriate feedback mechanism which couples the output signal to the control parameter that triggers the bifurcation. The concept can explain several important features of the auditory sensor such as the frequency selectivity, high sensitivity and the ability to respond to a wide range of amplitudes. It can also explain the intrinsic nonlinear nature of sound detection [13,14] and the occurrence of spontaneous sound emission by the inner ear [9,10]. Furthermore, self-tuned criticality provides a framework for understanding the role of noise in the detection mechanism. The amplification process, which involves a limited number of active elements, introduces stochastic fluctuations, which adds to those caused by Brownian motion. We show that the response to weak stimuli can take advantage of this background activity.

The proposed existence of a self-tuned Hopf bifurcation raises questions about the specific mechanisms involved: What is the physical basis of the dynamical system?

How is the self-tuning realized? It might be expected that different organisms have evolved different apparatus to implement the same general strategy. In this paper, we restrict our specific discussion to the more primitive cochleae of non-mammalian vertebrates. We propose a model of the hair cell of the inner ear which accords with data from a wide variety of physiological experiments. The model incorporates a physical mechanism which allows motor proteins to generate spontaneous oscillations [15]. We find that molecular motors such as dyneins in the kinocilium or myosins in the stereocilia are natural candidates for the force generators involved in the amplification of hair-bundle motion. Tension-gated transduction channels in the stereocilia serve primarily to detect this motion, but also have a second function: by admitting ions which regulate the motor protein activity, they provide the self-tuning mechanism.

## I. GENERIC ASPECTS

**Amplification and frequency filtering of a Hopf bifurcation.** We discuss the behavior of a dynamical system which is controlled by a parameter  $C$ . Above a critical value,  $C > C_c$ , the system is stable; for  $C < C_c$  it oscillates spontaneously. At the critical point (or Hopf bifurcation)  $C = C_c$  the system shows remarkable response and amplification properties which do not depend on the physical mechanism at the basis of the bifurcation. These generic properties can be described as follows. Since we are interested in the response to a periodic stimulus with frequency  $\nu = \omega/2\pi$ , we express the hair-bundle deflection  $x(t)$  by a Fourier series  $x(t) = \sum x_n e^{in\omega t}$  with complex amplitudes  $x_n = x_{-n}^*$ . In the vicinity of the bifurcation, the mode  $n = \pm 1$  is dominant and the response to an externally-applied sinusoidal stimulus force  $f(t) = f_1 e^{i\omega t} + f_{-1} e^{-i\omega t}$  can be expressed in terms of a systematic expansion in  $x_1$ . Symmetry arguments (see Appendix A) imply that the first nonlinear term is cubic:

$$f_1 = \mathcal{A} x_1 + \mathcal{B} |x_1|^2 x_1 + \dots \quad (1)$$

where  $\mathcal{A}(\omega, C)$  and  $\mathcal{B}(\omega, C)$  are two complex functions. The bifurcation point is characterized by the fact that  $\mathcal{A}$  vanishes for the critical frequency,  $\mathcal{A}(\omega_c, C_c) = 0$ . For  $C < C_c$  and no external force, the system oscillates with  $|x_1|^2 \simeq \Delta^2 (C_c - C)/C_c$ , where  $\Delta$  is a characteristic amplitude. For  $C = C_c$  the response to a stimulus at the critical frequency has amplitude

$$|x_1| \simeq |\mathcal{B}|^{-1/3} |f_1|^{1/3} \quad (2)$$

This represents an amplified response at the critical frequency with a gain

$$r = \frac{|x_1|}{|f_1|} \sim |f_1|^{-2/3} \quad (3)$$

that becomes arbitrarily large for small forces.

If the stimulus frequency differs from the critical frequency, the linear term in Eq. (1) is non-zero and can be expressed to first order as  $\mathcal{A}(\omega, C_c) \simeq A_1 (\omega - \omega_c)$ . The dramatic amplification of weak signals, implied by Eq. (3), is maintained as long as this term does not exceed the cubic term in Eq. (1). If the frequency mismatch increases such that  $|\omega - \omega_c| \gg |f_1|^{2/3} |\mathcal{B}|^{1/3} / |A_1|$ , the response becomes linear

$$|x_1| \simeq \frac{|f_1|}{|(\omega - \omega_c) A_1|} \quad (4)$$

i.e. the gain is independent of the strength of the stimulus.

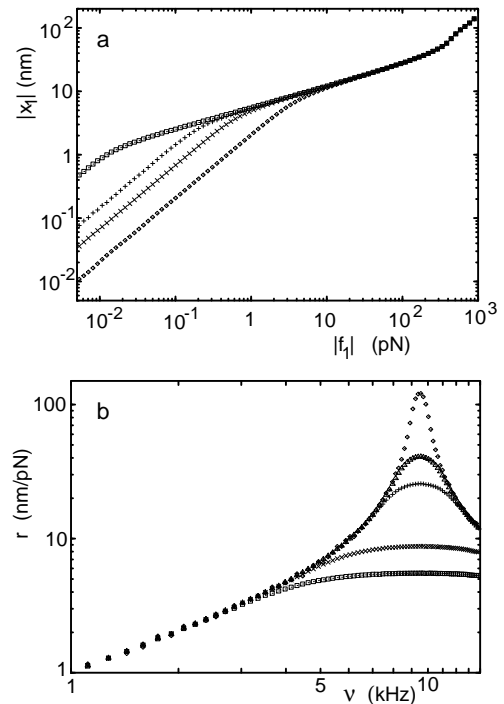


FIG. 1. Response to external forces near a Hopf bifurcation (a) Amplitude  $|x_1|$  as a function of force  $|f_1|$  at various driving frequencies  $\nu$  ( $\diamond$  2 kHz,  $\times$  5 kHz,  $\square$  10 kHz,  $+$  13 kHz). (b) Gain  $r$  as a function of frequency  $\nu$  for different amplitudes  $|f_1|$  ( $\diamond$  0.01 pN,  $\triangle$  0.05 pN,  $+$  0.1 pN,  $\times$  0.5 pN,  $\square$  1 pN). While the form of these curves is generic, the numerical values of force, amplitude and frequency depend on the physical nature of the dynamical system. The values given here correspond to the specific model of a hair cell discussed in the text, with parameters chosen to give a critical frequency of approximately 10 kHz.

Thus the Hopf resonance acts as a sharply tuned high-gain amplifier for weak stimuli, and as a low-gain filter for strong stimuli. This generic behavior is illustrated in Fig. 1 with data obtained by numerical simulation. Laser interferometry measurements of the motion of the basilar membrane, when the live cochlea is stimulated by pure tones, display strikingly similar features [16,17].

In particular, the peak response as a function of force amplitude has been demonstrated to obey a power law  $|x_1| \sim |f_1|^{0.4 \pm 0.2}$  [17]. This strongly suggests that the membrane is being driven by a dynamical system which is poised at a Hopf bifurcation.

**Self-tuned critical oscillations.** How does the system come to be so precisely balanced at the critical point?<sup>1</sup> The control parameter must be tuned to  $C \simeq C_c$ , otherwise the nonlinear amplification is lost. Moreover, the value of  $C_c$  differs for hair cells with different characteristic frequency. We propose a feedback mechanism which allows the dynamical system to operate *automatically* close to the bifurcation point, whatever its characteristic frequency. Without loss of generality, we assume that the control parameter decreases as long as the system does not oscillate. After some time, critical conditions are reached and spontaneous oscillations ensue. The onset of oscillations triggers an increase of the control parameter which tends to restore stability. Hence the system converges to an operating point close to the bifurcation point. To illustrate this general idea, we consider the following simple feedback which changes  $C$  in response to deflections  $x$ :

$$\frac{1}{C} \frac{\partial C}{\partial t} = \frac{1}{\tau} \left( \frac{x^2}{\delta^2} - 1 \right) \quad (5)$$

where  $\delta$  is a typical amplitude. If no external force is applied, this feedback, after a relaxation time  $\tau$ , tunes the control parameter to a value  $C_\delta$  for which spontaneous oscillations with  $|x_1| \simeq \delta$  occur. If  $\delta$  is small compared to the characteristic amplitude  $\Delta$ , this is on the oscillating side close to the bifurcation,  $|C_\delta - C_c|/C_c \simeq (\delta/\Delta)^2$ . Two modes of signal detection are possible: (i) For transient stimuli short compared to  $\tau$  the system operates at  $C_\delta$ . The amplitude  $|x_1|$  shows the characteristic nonlinear response discussed above. (ii) For stimuli sustained over longer times, self-tuning maintains  $|x_1| \simeq \delta$  constant for different stimulus amplitudes. This effect of the feedback represents a perfect adaptation mechanism. However, in the presence of noise, phase-locking of the response (to be discussed later) occurs as soon as an external stimulus is applied, and this can be detected.

## II. MODEL

**Mechanosensitivity and self-tuning mechanism provided by transduction channels.** We demonstrate the general principles introduced above by devising a specific model for the amplification of acoustic stimuli by hair bundles in non-mammalian vertebrates. A

schematic representation of a hair bundle is shown in Fig. 2. It consists of several stereocilia and a single kinocilium [19,20]. Transduction of hair bundle deflection to a chemical signal occurs via channels located near the tip of each stereocilium. Tip links which connect neighboring stereocilia are believed to be the gating springs of the transduction channels. If the hair bundle is deflected, tension in the tip links triggers the opening of the channels. The subsequent influx of ions (principally  $K^+$ , but also  $Ca^{2+}$ ) causes a corresponding change of the membrane potential of the hair cell which, in turn, generates a nervous signal.

The mechanosensor can be used for self-tuning, as well as signal detection. Many physiological processes are regulated by ionic concentrations, so it is natural to identify the  $Ca^{2+}$  concentration with the control parameter  $C$ . We assume that  $C$  decreases if the transduction channels are closed, owing to the action of pumps in the cell membrane. When the hair bundle is deflected by  $x$ , the transduction channels open with probability  $P_o(x)$ . We therefore characterize the mechanosensor by the equation

$$\frac{\partial C}{\partial t} = -\frac{C}{\tau} + J_o P_o(x) \quad (6)$$

where  $J_o$  is the  $Ca^{2+}$  flux through open transduction channels. Note that this equation provides self-tuning. In this case it replaces the more simple but less realistic Eq. (5). For our numerical examples, we use a two-state model for the channels with

$$P_o(x) = \frac{1}{1 + A e^{-x/\delta}} \quad (7)$$

where  $(1 + A)^{-1} \ll 1$  is the probability that a channel is open when the hair cell is quiescent and  $\delta$  is the characteristic amplitude of motion to which the system is sensitive. For a sufficiently long relaxation time  $\tau$ , the slow variation  $C_0$  of  $C \simeq C_0(t) + C_1 e^{i\omega t}$  can be separated from the small-amplitude oscillations, giving

$$\partial_t C_0 \simeq -\frac{C_0}{\tau} + J_o \tilde{P}_o(|x_1|^2) \quad (8)$$

where  $\tilde{P}_o = \int_0^{1/\nu} dt P_o(x_1 e^{i\omega t} + x_{-1} e^{-i\omega t})$  is the averaged probability of channel opening in the presence of oscillations, which increases monotonically with their amplitude  $x_1$ . For physically relevant parameter values, the system reaches a steady state close to the bifurcation point, independent of the initial value of  $C$ .

**Oscillations generated by molecular motors.** We still have to specify the nature and location of the oscillator within the hair bundle. It has been suggested that the transduction channels might be the source of the instability [7,12]; or, that myosin motors in the stereocilia might generate the force necessary to move the bundle [21,22]. We propose a third possibility: the kinocilium could vibrate using its internal dynein motors. Recently,

<sup>1</sup>Self-tuning to a coexistence point has been discussed previously in certain dynamic first-order transitions [18].

a simple physical mechanism has been proposed which allows motor proteins operating in collections to generate spontaneous oscillations by traversing a Hopf bifurcation [15,23]. Typically, motors move along cytoskeletal filaments and elastic elements oppose this motion. In this case, two possibilities exist: The system either reaches a stable balance between opposing forces, or it oscillates around the balanced state. Three time scales characterize this behavior: The relaxation time  $\lambda/K$  of passive relaxation, where  $\lambda$  is the total friction and  $K$  is the elastic modulus; and the times  $\omega_1^{-1}$  and  $\omega_2^{-1}$ , where  $\omega_1$  is the kinetic rate at which a motor detaches from a filament, and  $\omega_2$  is the attachment rate. An explicit solution of a simple model is derived in Appendix B. We find that for an appropriate value of a control parameter  $C$ , which is related to the ratio  $\omega_1/\omega_2$ , a Hopf bifurcation occurs with critical frequency

$$\omega_c \simeq \left( \frac{K\alpha}{\lambda} \right)^{1/2}, \quad (9)$$

which is the geometric mean of the passive relaxation rate  $K/\lambda$  and the typical ATP hydrolysis rate  $\alpha = \omega_1 + \omega_2$ . The above identification of  $C$  with the  $\text{Ca}^{2+}$  concentration is consistent with the fact that  $\text{Ca}^{2+}$  regulates motor protein activity [24]. The system oscillates if the elastic modulus does not exceed a maximal value  $K_{\max} \simeq k_0 N$ , where  $k_0$  is the crossbridge elasticity of a motor and  $N$  is the total number of motors. The maximal frequency, obtained when  $K = K_{\max}$ , can be significantly higher than the ATP hydrolysis rate  $\alpha$ .

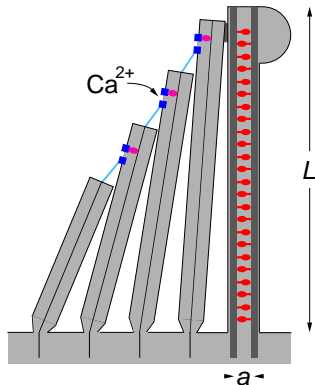


FIG. 2. A hair bundle consists of a single kinocilium and tens to hundreds of stereocilia. The kinocilium contains dynein motors (red). The stereocilia contain transduction channels (blue) which are gated by the tension in the tip links (cyan); the steady-state tension is maintained constant by adaptation motors (magenta). In our model, the kinocilium is the active part of the mechanoreceptor and the stereocilia act as the detection apparatus. Feedback control of the active amplification process involves the influx of  $\text{Ca}^{2+}$  ions through the transduction channels; the ions diffuse into the kinocilium and regulate the generation of force by the motor proteins.

**Characteristic frequency of a vibrating kinocilium.** The kinocilium is a true cilium containing a cylindrical arrangement of microtubule doublets and dynein motors. Since cilia have the well-established tendency to beat and vibrate with frequencies from tens of Hz up to at least 1 kHz [25,26], the kinocilium is a natural candidate to be responsible for the Hopf bifurcation. A simple two-dimensional model can be used to discuss the main physical properties of a vibrating cilium near a Hopf bifurcation [27]. In this model, motors induce the bending of a pair of elastic filaments separated by a distance  $a$  (corresponding to the distance between neighboring microtubule doublets in the axoneme). An isolated kinocilium of length  $L$  and bending rigidity  $\kappa$ , fixed at the basal end but free at its tip, will vibrate in a wave-like mode with wavelength  $\Lambda \simeq 4L$ . A typical displacement  $z$  of the motors along the filaments leads to bending of the filament pair and a deflection of the tip by a distance  $x \simeq zL/a$ . The elastic bending energy is of order  $(\kappa/L^3)x^2 \simeq (\kappa/a^2L)z^2$ . Therefore, the total elastic modulus experienced by the motors is given by

$$K \simeq \frac{\kappa}{La^2}. \quad (10)$$

The viscous energy dissipation per unit time due to motion of the kinocilium is of order  $\eta L(\partial_t x)^2 \simeq (\eta L^3/a^2)(\partial_t z)^2$ . Therefore, the total friction experienced by the motors can be written as

$$\lambda \simeq \frac{\eta L^3}{a^2} + \lambda_0 \rho L, \quad (11)$$

where  $\lambda_0$  describes the dissipation within the kinocilium per motor and  $\rho = N/L$  denotes the number of dynein motors per unit length along the axoneme. If internal friction can be neglected, i.e. if  $L \gg L_0 = (\lambda_0 a^2 \rho / \eta)^{1/2}$ , the frequency of a vibrating cilium at the bifurcation point is given by

$$\omega_c \simeq \left( \frac{\kappa \alpha}{\eta} \right)^{1/2} \frac{1}{L^2}. \quad (12)$$

Using typical values  $\lambda_0 \simeq 10^{-9} \text{ kg/s}$ ,  $a \simeq 20 \text{ nm}$ ,  $\rho \simeq 5 \cdot 10^8 \text{ m}^{-1}$  and  $\eta \simeq 10^{-3} \text{ kg/ms}$ , we find  $L_0 \simeq 200 \text{ nm}$ , shorter than typical kinocilia. Using  $\alpha \simeq 10^3 \text{ s}^{-1}$ ,  $k_0 \simeq 10^{-3} \text{ N/m}$  and  $\kappa \simeq 4 \cdot 10^{-22} \text{ Nm}^2$  (the bending rigidity of 20 microtubules), the frequency range between 100 Hz and 10 kHz can naturally be spanned by changing the length of the kinocilium between  $1 \mu\text{m}$  and  $10 \mu\text{m}$ .

The above argument neglects the contribution of the stereocilia to elasticity and motion. The elastic response of stereocilia to hair bundle deflections has been measured [6,28]. It can be well described by an angular spring at the base of each stereocilium which contributes an elastic energy per stereocilium of the order of  $k_s(x/L)^2$ , where  $k_s$  is an angular elastic modulus. The kinocilium

length  $L$  in a hair bundle is approximately inversely proportional to the number  $N_s$  of stereocilia [19], and we write  $N_s \simeq l_s/L$ , where  $l_s \simeq 10^{-4}$  m is the total length of stereocilia. With this assumption, we find an additional elastic modulus

$$K_s \simeq \frac{l_s k_s}{La^2} \quad (13)$$

contributed by the stereocilia to  $K$ . The contribution of stereocilia to the friction coefficient  $\lambda$  can be estimated as

$$\lambda_s \simeq \eta l_s L^2 / a^2 \quad (14)$$

The measured value of  $k_s$  [28] indicates that  $K_s$  dominates the contribution to  $K$  given by Eq. (10). Similarly, since  $l_s > L$ ,  $\lambda_s$  should dominate friction. In this case, we expect

$$\omega_c \simeq \left( \frac{k_s \alpha}{\eta L^3} \right)^{1/2} \quad (15)$$

and the range of frequencies is somewhat reduced.

If the stiffness of the ensemble of stereocilia greatly exceeds that of the kinocilium, a new situation arises. Since the kinocilium is attached to the stereocilia at its tip [20], movement of the tip is strongly reduced and the kinocilium preferentially vibrates in a mode with wavelength  $\Lambda \simeq 2L$  for which the relation given by Eq. (12) is again valid.

**Adaptation motors.** Finally, we note that in order to obtain a robust self-tuning, the feedback mechanism must be sensitive only to the oscillation amplitude  $x_1$  and not to a stationary displacement  $x_0$ ; we assumed in Eq. (8) that  $\tilde{P}_o$  is independent of  $x_0$ . The transduction mechanism of stereocilia and their tension-gated channels does indeed have this property: It is well known that an ATP-dependent adaptation mechanism [29] exists which removes the dependence of the channel current on a constant displacement  $x_0$ . It is widely believed that this adaptation involves the motion of myosin motors, which maintains constant the steady-state tension in the tip links that control the transduction channels [30]. Therefore, the stereociliar transduction mechanism has precisely the required properties to be used as a feedback signal for self-tuning the bifurcation.

### III. SIMULATION

The above analysis does not include the effects of noise. Brownian motion is one source of fluctuations in the movement of the hair bundle [31]. Another source of noise is caused by stochastic fluctuations in motor protein force as dynein molecules bind to, and detach from the microtubules in the kinocilium. In order to investigate the consequences of this randomness, we performed

a Monte Carlo simulation of the two-state model described in [15], using a realistic number of motor proteins. The motors, when attached, experienced a potential of amplitude  $U$  and period  $l$  (the corresponding crossbridge elasticity is  $k_0 = U/l^2$ ). The attachment rate was constant and independent of position,  $\omega_2 = \alpha$ . Detachment was localized to a region of width  $0.1l$ , centred on the potential minimum and the detachment rate  $\omega_1$  was regulated by the  $\text{Ca}^{2+}$  concentration  $C$ . We chose  $\omega_1/\omega_2 = (C_q/C)^3$ , where  $C_q$  is the steady-state  $\text{Ca}^{2+}$  concentration in a quiescent hair cell; the precise functional dependence is unimportant as long as  $\omega_1/\omega_2$  decreases monotonically with increasing  $C$  in a fairly sensitive way. We simulated systems with  $N = 1000$ -4000 motors, representing hair cells with different kinocilium length and stereociliary number.

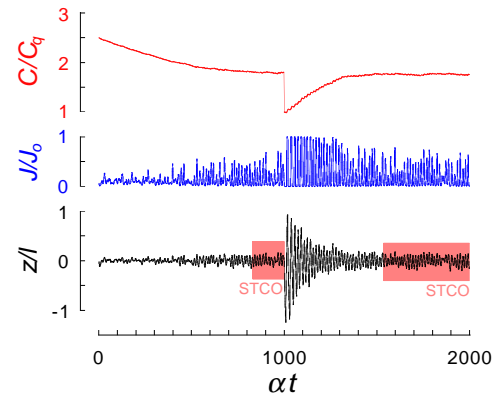


FIG. 3. Self-tuning of a hair bundle. If the  $\text{Ca}^{2+}$  concentration  $C$  within the cell is artificially high, the hair bundle is initially quiescent; but as  $\text{Ca}^{2+}$  ions are pumped from the cell, it gradually begins to oscillate with small amplitude. If  $C$  is suddenly artificially lowered, the hair bundle becomes unstable and executes high-amplitude spontaneous oscillations. Since these movements open the transduction channels, the influx  $J$  of  $\text{Ca}^{2+}$  ions increases; the consequent change in  $C$  regulates the motors and diminishes the amplitude of the oscillation until it almost disappears. In the steady state, the bundle executes *self-tuned critical oscillations* (STCO). For this simulation, we assumed that the probability of transduction channels opening was  $P_o(z) = (1 + 10e^{-20z/l})^{-1}$ , where  $z$  is the motor displacement, and that the time constant for equilibration of the  $\text{Ca}^{2+}$  concentration was  $\tau = 1000/\alpha$ .

**Self-tuning and the characteristic frequency of spontaneous oscillations.** The self-tuning of a hair cell to the vicinity of the bifurcation, where small-amplitude spontaneous oscillations occur, is demonstrated in Fig. 3. When a change of the internal  $\text{Ca}^{2+}$  concentration is imposed, the system is transiently perturbed; but after an interval of time of order  $\tau$ , it returns to the same steady state. Hair cells with different numbers of motors acquire different internal concentrations of  $\text{Ca}^{2+}$ , in order to adjust the motor detachment rate in such a way

that the system approaches the critical point. The spontaneous oscillations of three different hair bundles are shown in Fig. 4. Note that the characteristic frequency is approximately proportional to the inverse-square of the number of motors, as expected from Eq. (12), and that it can exceed the typical ATP cycle rate  $\alpha$  when the total number of motors is small (short kinocilium). All three hair cells execute spontaneous oscillations with a similar amplitude, as expected from our arguments above. However, the noise introduces a significant new effect: The oscillations are irregular. The incoherence of the phase of the oscillation is evident in the Fourier transform of the displacement, which exhibits a broad peak centred on the characteristic frequency.

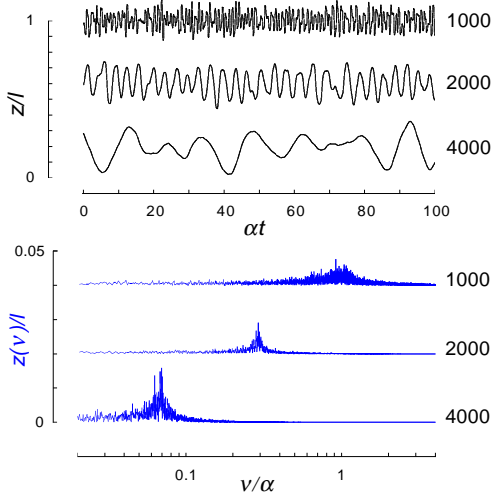


FIG. 4. Self-tuned critical oscillations of systems comprising  $N = 1000, 2000$  and  $4000$  motors. In each case, the oscillation has small amplitude  $z \simeq 0.1l$  and is irregular, as can be seen from the broadness of the Fourier spectrum. For these simulations we chose parameters  $k_0/\lambda\alpha = 4 \cdot 10^7 N^{-3}$  and  $K/\lambda\alpha = 4 \cdot 10^{13} N^{-4}$ , which correspond with the scaling dependence of the spring constant and friction coefficient on kinocilium length in Eqs. (10-11), and also with the order of magnitude estimates of the physical parameters, given in the text.

**Dynamic response to a tone at the characteristic frequency.** The response of a self-tuned hair bundle to a sinusoidal force with a frequency approximately equal to the bundle's characteristic frequency is illustrated in Fig. 5. For weak stimuli, the amplitude of the oscillation does *not* increase with the amplitude  $|f_1|$  of the applied force; this is because the small response to the stimulus is masked by the noisy, spontaneous motion. Instead, the *phase* of the hair-bundle oscillation becomes more regular; as it does so, a peak emerges from the Fourier spectrum at the driving frequency. The height of the peak grows approximately as  $|f_1|^{1/3}$  for intermediate values of  $|f_1|$ , and approximately linearly for very weak stimuli, and also for very strong stimuli (for which the

response is essentially passive). Thus the Fourier component of the hair-bundle displacement at the driving frequency responds to the stimulus in the generic manner discussed above.

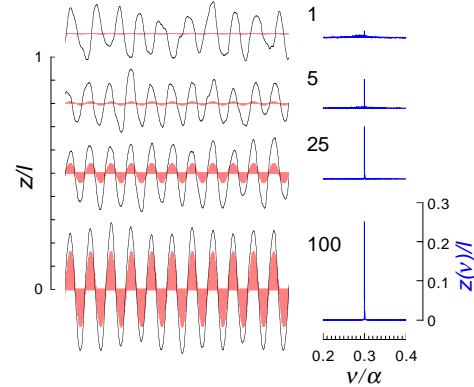


FIG. 5. Response of a system with  $N = 2000$  motors to a sinusoidal force at frequency  $\nu = 0.3\alpha$ , close to the hair bundle's characteristic frequency. Curves are marked by the dimensionless amplitude of the force,  $|f_1|/f_{mot}$ , where  $f_{mot} = U/l$  is the force produced by a motor molecule. Note that a force equal to that of a single motor is sufficient to elicit a response in the Fourier spectrum. Curves shaded red are the responses of an equivalent, passive hair bundle (i.e. a bundle with identical mechanical properties but no force generators).

**Phase-locking of the nervous signal.** The flow of ions through the transduction channels depolarizes the cell membrane which, in turn, opens voltage-gated channels at the base of the hair cell and generates a synaptic current [1]. This sequence of events happens fast enough for variations at the synapse faithfully to reflect the hair-bundle motion at frequencies below 1 kHz. Information about the auditory stimulus is subsequently passed along the auditory nerve in the form of a spike train. Simplifying this transduction process, we assume that a spike is elicited whenever the transduction channel current  $J$  passes a threshold value of  $0.5J_0$ . The resulting nervous response is shown in Fig. 6. In the absence of a stimulus, the self-tuned critical oscillations of the bundle cause the nerve to fire stochastically, at a low rate. When a weak sinusoidal stimulus is applied at the characteristic frequency, the firing rate does not increase above the spontaneous rate, but the spike train becomes detectably phase-locked to the stimulus. The degree of phase-locking increases rapidly as the amplitude of the stimulus increases, reflecting the growing regularity of the hair-bundle motion. It is only when the neural response is almost completely phase-locked that the firing rate begins to rise. Eventually, for strong stimuli, the spike rate saturates at the stimulus frequency. This be-



havior is strikingly similar to that which is observed experimentally. In particular, it is well known that the threshold for phase-locking in the auditory nerve fiber is 10-20 dB lower than the threshold at which the firing rate begins to rise [32,33].

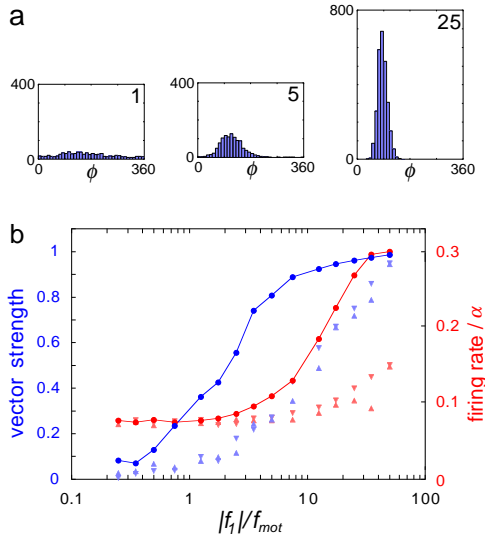


FIG. 6. (a) Histogram of the phase  $\phi$  of the driving force at the instants when nervous spikes are generated, for various values of the force amplitude (marked by the value of  $|f_1|/f_{mot}$ ). (b) Degree of phase-locking (blue; expressed as the vector strength  $\int d\phi p(\phi)e^{i\phi}$ ) and firing rate (red), as a function of the driving force. The frequency selectivity of the bundle can be appreciated by comparing the neural response to a stimulus with frequency close to the characteristic frequency,  $\nu = 0.3\alpha$  ( $\bullet$ ), with the response to other frequencies,  $\nu = 0.15\alpha$  ( $\nabla$ ) and  $\nu = 0.6\alpha$  ( $\Delta$ ).

#### IV. DISCUSSION

The self-tuned critical oscillator which we have introduced as a system for signal detection has characteristic amplification properties which are generic and do not depend on the choice of a specific model. The oscillation frequency, however, depends on the physical mechanism involved. In our model of non-mammalian hair cells, the frequency is determined by the geometry of the hair bundle. A simple morphological gradient along the basilar membrane would endow the ear with the ability to analyze a wide range of frequencies. Experimentally, it is well established that the height of hair bundles progressively increases along the cochlea, and that concurrently the characteristic frequency of the hair cells declines [19,34]. Our proposition that the kinocilium is likely to play an active role in non-mammalian vertebrate hair cells suggests experiments which study the motility of the kinocilium and its potential for generating oscillations. If the kinocilium is the only source of oscillations, its removal should suppress hair-bundle vibrations. If

the self-tuning mechanism is removed instead (by cutting the tip links, for example) our model predicts that the kinocilium should exhibit stronger spontaneous oscillations. Careful control of the extracellular ion concentrations, such as  $\text{Ca}^{2+}$  would be essential in such experiments.

The simulations of our model reveal how a hair bundle can achieve its remarkable sensitivity to weak stimuli. By profiting from the periodicity of a sinusoidal input, and measuring phase-locking rather than the amplitude of response, the mechanosensor can detect forces considerably weaker than those exerted by a single molecular motor (if the bundle were a simple, passive structure, its response to such forces would be smaller than its Brownian motion). An important implication of this detection mechanism is that even though the hair cell selects a certain frequency, the signal must still be encoded by the interval between spikes elicited in the auditory nerve. Paradoxically, the stochastic noise caused by the motor proteins serves a useful purpose. It ensures that the self-tuned critical oscillations of the hair bundle are incoherent, so that the pattern of spontaneous firing in the nerve is irregular. Against this background, the regular response to a periodic stimulus can easily be detected.<sup>2</sup>

Another beneficial feature of noise arises from the fact that weak stimuli do not increase the amplitude of oscillation above the spontaneous amplitude. Thus the  $\text{Ca}^{2+}$  concentration remains constant, the hair bundle stays in the critical regime, and active amplification can be sustained indefinitely. Stronger stimuli cause the system to drift away from the critical point, so that the degree of amplification diminishes over time. It is well known that both the perception of loudness [35] and the firing rate of the auditory nerve [36] decrease over a period of a few seconds, when a stimulus of moderate intensity is maintained. This phenomenon, which is usually referred to as ‘adaptation’, is consistent with our self-tuning mechanism. Following the sustained presentation of a loud stimulus, the spontaneous firing rate diminishes and the threshold to weak stimuli is augmented [36]. Such ‘fatigue’ is also accounted for by our self-tuning mechanism.

Since self-tuning positions the system slightly on the oscillating side of the critical point, self-tuned criticality provides a natural explanation for otoacoustic emissions [9,10]. In its normal working state, the inner ear would generate faint sounds with a broad range of frequencies. If the feedback mechanism were to fail in certain cells, the spontaneous oscillations could become large enough for distinct tones to be emitted.

A self-tuned Hopf bifurcation is ideal for sound detection because it provides sharp frequency selectivity and a

<sup>2</sup>The benefits of noise have been discussed in a variety of situations such as those involving stochastic resonance [37].

nonlinear gain which compresses a wide range of stimulus intensities into a narrow range of response. We therefore believe that the concept applies to all vertebrate hearing systems, and potentially to other mechanoreceptor systems. Kinocilia are typically absent in mammalian cochlea, and we suggest that their force-generating role has been assumed by the outer hair cells. Self-tuning of these motile cells might be realized by a mechanism similar to that presented here, using transduction channels in their hair bundles. It could, however, work very differently; for example, it might involve feedback from the inner hair cells, via the efferent nervous system.

Tuning to the proximity of a critical point is likely to be a general strategy adopted by sensory systems. Simple molecular receptors [38], as well as the physiological sensors of higher organisms, can enhance their response to weak stimuli in this way. We propose that the physics of self-tuned criticality is the ‘central science of transducer physiology’ spoken of by Delbrück [39].

**Acknowledgements:** We thank P. Martin and C. Petit for useful discussions, and A.F. Huxley for referring us to the work of T. Gold. T. Duke is grateful for the hospitality of Institut Curie and the Niels Bohr Institute, and acknowledges the support of the Royal Society. After submission of our manuscript we learned that Eguiluz, Ospeck, Choe, Hudspeth and Magnasco have independently described the generic response of a system near a Hopf bifurcation; we thank them for communicating their unpublished results.

## APPENDIX A: GENERIC BEHAVIOR AT A HOPF-BIFURCATION

### 1. Nonlinear relation between periodic stimulus and displacements

We are interested in the response  $x(t)$  of a nonlinear system to a periodic stimulus force  $f(t)$ . If only one frequency  $\nu = \omega/2\pi$  is present we use the Fourier expansions

$$f(t) = \sum_{n=-\infty}^{\infty} f_n e^{in\omega t} \quad (\text{A1})$$

$$x(t) = \sum_{n=-\infty}^{\infty} x_n e^{in\omega t} \quad , \quad (\text{A2})$$

where the complex coefficients  $x_n$  and  $f_n$  obey  $x_n = x_{-n}^*$  and  $f_n = f_{-n}^*$ . This representation implies that we focus on the limit cycle solution and ignore all transient relaxation phenomena. We consider the class of systems for which the force at a given time depends in a nonlinear way on the history of the displacements  $x(t)$  alone; as we will discuss in section D more complex cases do not

change the basic properties. In this situation, the relation between  $x$  and  $f$  can be expressed as a systematic expansion of the force amplitudes  $f_n$  in the amplitudes  $x_n$ :

$$f_k = F_{kl}^{(1)} x_l + F_{klm}^{(2)} x_l x_m + F_{klmn}^{(3)} x_l x_m x_n + O(x^4) \quad , \quad (\text{A3})$$

where the expansion coefficients  $F_{k,k_1,\dots,k_n}^{(n)}$  are symmetric with respect to permutations of the indices  $k_1 \dots k_n$ . The limit cycle solutions are invariant with respect to translations in time  $t \rightarrow t + \Delta t$ . Under these transformations the amplitudes change as  $x_n \rightarrow x_n e^{in\omega\Delta t}$  and  $f_n \rightarrow f_n e^{in\omega\Delta t}$ . Inspection of Eq. (A3) shows that the time translation symmetry allows only for those terms  $F_{k,k_1,\dots,k_n}^{(n)} x_{k_1} \dots x_{k_n}$  for which  $k = k_1 + \dots + k_n$ . For all other cases  $F_{k,k_1,\dots,k_n}^{(n)}$  must vanish which significantly restricts the number of terms.

### 2. Hopf bifurcation

The nonlinear system exhibits spontaneous oscillations and a Hopf-bifurcation if nontrivial solutions to Eq. (A3) with  $x_n \neq 0$  exist in the case where all  $f_k = 0$ , i.e. if no stimulus force is applied. Without loss of generality, we consider here an instability of the mode  $x_1$ . In this case, the dominant terms allowed by symmetry read ( $f_k = 0$ )

$$0 \simeq F_{11}^{(1)} x_1 + 2F_{1,2,-1}^{(2)} x_{-1} x_2 + 6F_{1,1,1,-1}^{(3)} x_1^2 x_{-1} + 6F_{1,1,2,-2}^{(3)} x_2 x_{-2} x_1 \quad (\text{A4})$$

$$0 \simeq F_{22}^{(2)} x_2 + 2F_{211}^{(2)} x_1^2 \quad . \quad (\text{A5})$$

Eq. (A5) determines  $x_2 \simeq -2(F_{211}^{(2)}/F_{22}^{(2)})x_1^2$ . Inserting this relation in Eq. (A4), we obtain to lowest order

$$0 \simeq \mathcal{A}x_1 + \mathcal{B}|x_1|^2 x_1 \quad , \quad (\text{A6})$$

where  $\mathcal{A} \equiv F_{11}^{(1)}$  and  $\mathcal{B} \equiv 3F_{1,1,1,-1}^{(3)} - 4F_{211}^{(2)}F_{1,2,-1}^{(2)}/F_{22}^{(2)}$ .

The coefficients  $\mathcal{A}(\omega, C)$  and  $\mathcal{B}(\omega, C)$  are complex and in general depend on frequency  $\omega$  and a control parameter which we denote by  $C$ . A Hopf bifurcation occurs at a critical point  $C = C_c$  at which  $\mathcal{A}$  vanishes for a frequency  $\omega_c$ , i.e.  $\mathcal{A}(\omega_c, C_c) = 0$ . This can be demonstrated as follows: A spontaneously oscillating solution satisfies

$$|x_1|^2 = -\frac{\mathcal{A}}{\mathcal{B}} \quad (\text{A7})$$

Note, that such a solution can only exist if  $\mathcal{A}/\mathcal{B}$  is real and negative. At the bifurcation point,  $\mathcal{A} = 0$  and  $\mathcal{A}/\mathcal{B}$  is therefore real for  $\omega = \omega_c$ , however the corresponding amplitude  $|x_1|^2$  vanishes. In the vicinity of this point we expect to find solutions with finite amplitude. We use the expansion



$$\mathcal{A}(\omega, C) \simeq (\omega - \omega_c)A_1 + (C - C_c)A_2 \quad (\text{A8})$$

where  $A_1$  and  $A_2$  are complex coefficients and we neglect higher order terms. Spontaneous oscillating solutions exist only if  $\mathcal{A}/\mathcal{B}$  is real. This condition is satisfied for a particular frequency  $\omega = \omega_s$  with

$$\omega_s = \omega_c + \frac{\text{Im}(A_2/\mathcal{B})}{\text{Im}(A_1/\mathcal{B})}(C_c - C) \quad (\text{A9})$$

The ratio  $-\mathcal{A}/\mathcal{B}$  at this frequency  $\omega_s$  changes sign for  $C = C_c$ ; here we assume without loss of generality that it is positive for  $C < C_c$ . In this case, the system oscillates spontaneously with an amplitude which according to Eq. (A7) behaves as  $|x_1|^2 = \Delta^2(C_c - C)/C_c$ , where

$$\Delta^2 = C_c \left( \text{Re}(A_2/\mathcal{B}) - \text{Re}(A_1/\mathcal{B}) \frac{\text{Im}(A_2/\mathcal{B})}{\text{Im}(A_1/\mathcal{B})} \right) \quad (\text{A10})$$

is a typical amplitude. We have thus demonstrated that Eq. (A6) characterizes a Hopf-bifurcation if the complex coefficient  $\mathcal{A}$  vanishes at a critical point  $C_c$  for a critical frequency  $\omega_c$ .

### 3. Amplified response to sinusoidal stimuli

If a sinusoidal stimulus  $f(t) = f_1 e^{i\omega t} + f_{-1} e^{-i\omega t}$ , for which all  $f_n$  with  $n \neq \pm 1$  vanish, Eq. (A6) becomes

$$f_1 \simeq \mathcal{A}x_1 + \mathcal{B}|x_1|^2 x_1 \quad (\text{A11})$$

We consider a system that is tuned exactly to the bifurcation,  $C = C_c$ . In this situation spontaneous oscillations do not occur and  $\mathcal{A} = (\omega - \omega_c)A_1$ . If the imposed frequency is equal to the critical frequency  $\omega = \omega_c$ , the coefficient  $\mathcal{A}$  vanishes and we can solve Eq. (A11) for  $|x_1|$  to find the nonlinear response

$$|x_1| \simeq |\mathcal{B}|^{-1/3} |f_1|^{1/3} \quad (\text{A12})$$

as a function of the force amplitude  $|f_1|$ . This behavior represents an amplified response with a gain

$$r = \frac{|x_1|}{|f_1|} \sim |f_1|^{-2/3} \quad (\text{A13})$$

that becomes arbitrarily large for small forces. If the frequency  $\omega$  is different from  $\omega_c$ , this nonlinear response still holds as long as the linear term in Eq. (A11) is small compared to the cubic term and can be neglected. This is the case if  $|x_1|^2 \gg |\mathcal{A}/\mathcal{B}| = |\omega - \omega_c| |A_1/\mathcal{B}|$ . Therefore, the nonlinear regime characterized by Eq. (A12) holds for sufficiently large force amplitudes,  $|f_1| \gg |(\omega - \omega_c)A_1|^{3/2}/|\mathcal{B}|^{1/2}$ , or if the frequency is sufficiently close to the critical frequency,  $|\omega - \omega_c| \ll |f_1|^{2/3} |\mathcal{B}|^{1/3}/|A_1|$ .

If the frequency mismatch  $|\omega - \omega_c|$  becomes large, or if forces  $|f_1|$  are small, a new regime occurs for which

the linear term in (A11) dominates. In this regime, the response is linear,

$$|x_1| \simeq \frac{|f_1|}{|(\omega - \omega_c)A_1|} \quad (\text{A14})$$

and the gain is constant. This is a passive response if the stimulus frequency is too far from the critical frequency.

### 4. Additional remarks

The above derivation is based on an expansion (A3) in the displacements  $x_n$ . This excludes some nonlinearities in the force which can lead to additional nonlinear terms in Eq. (A11). The most general form of Eq. (A11) is

$$f_1 \simeq \mathcal{A}x_1 + \mathcal{B}|x_1|^2 x_1 + \mathcal{C}x_1|f_1|^2 + \mathcal{D}x_{-1}f_1^2 + \mathcal{E}|x_1|^2 f_1 + \mathcal{F}x_1^2 f_{-1} + \mathcal{G}|f_1|^2 f_1 \quad (\text{A15})$$

However, for small forces  $f_1$  and small amplitudes  $x_1$ , the results derived above are not affected. The regime of nonlinear response  $|f_1| \sim |x_1|^3$ , as well as the linear response regime  $|f_1| \sim |x_1|$  still exist. If  $|f_1| \sim |x_1|$ , the nonlinear terms in  $f_1$  renormalize the third order term, which in this regime is negligible. If  $|f_1| \sim |x_1|^3$ , the nonlinear terms in  $f_1$  are of even higher order and can be neglected.

## APPENDIX B: OSCILLATIONS GENERATED BY MOLECULAR MOTORS

### 1. Two state model

The two state model describes force-generation as a result of transitions between two states, a bound state and a detached state of a motor and its track filament. The interaction between a motor at position  $z$  along the filament in states 1 and 2 is characterized by two periodic potentials  $W_1(z) = W_1(z + l)$  and  $W_2(z) = W_2(z + l)$  where  $l$  is the period. We introduce the relative position  $\xi = z \bmod l$  with respect to the potential period. Detachment and attachment rates are denoted  $\omega_1(\xi)$  and  $\omega_2(\xi)$ , respectively. Oscillations can occur in this model if a large number  $N$  of motors move collectively against an external elastic element of modulus  $K$ .

We introduce the probability  $P_1(\xi)$  and  $P_2(\xi)$  of finding a motor bound at position  $\xi$  in state 1 or 2, which satisfy the normalization condition

$$\int_0^l d\xi (P_1 + P_2) = 1 \quad (\text{B1})$$

For a large number of motors collectively moving with the same velocity  $v$  the dynamic equations read

$$\partial_t P_1 + v \partial_\xi P_1 = -\omega_1 P_1 + \omega_2 P_2 \quad (\text{B2})$$

$$\partial_t P_2 + v \partial_\xi P_2 = \omega_1 P_1 - \omega_2 P_2 \quad (\text{B3})$$

The velocity  $v$  is determined by the force-balance condition

$$f = \lambda v + Kz + N \int_0^l d\xi (P_1 \partial_\xi W_1 + P_2 \partial_\xi W_2) \quad (\text{B4})$$

where  $\lambda$  is a friction coefficient describing the total friction and  $z$  is the displacement of the motors,  $\partial_t z = v$ . For an incommensurate arrangement of motors with respect to the track filament and a large number  $N$  of motors,  $P_1(\xi) + P_2(\xi) = 1/l$  and the equations of motions simplify:

$$\partial_t P + v \partial_\xi P = -(\omega_1 + \omega_2)P + \omega_2/l, \quad (\text{B5})$$

where we denote for simplicity  $P(\xi) = P_1(\xi)$ .

We discuss a simple choice for the potentials and transition rates for which the Hopf bifurcation is easy to determine analytically. We consider the potential

$$W_1(\xi) = U \cos(2\pi\xi/l) \quad (\text{B6})$$

with amplitude  $U$ , and the potential  $W_2$  to be constant. The transition rates are chosen to be periodic functions

$$\omega_1(\xi) = \beta - \beta \cos(2\pi\xi/l) \quad (\text{B7})$$

$$\omega_2(\xi) = \alpha - \beta + \beta \cos(2\pi\xi/l) \quad (\text{B8})$$

parameterized by two coefficients  $\alpha$  and  $\beta$ . With this choice,

$$\omega_1(\xi) + \omega_2(\xi) = \alpha \quad (\text{B9})$$

is constant and the fact that  $\omega_1$  and  $\omega_2$  are positive restricts  $\beta$  to the interval  $0 \leq \beta \leq \alpha/2$ .

## 2. Linear response function

In order to determine the linear coefficient  $\mathcal{A}$  which determines the stability of the system, we look for small amplitude oscillations close to the resting state with  $v = 0$ . We write

$$P \simeq p_0 + p_1 e^{i\omega t} \quad (\text{B10})$$

$$f \simeq f_1 e^{i\omega t} \quad (\text{B11})$$

$$z \simeq z_1 e^{i\omega t} \quad (\text{B12})$$

where  $p_0 = \omega_2/\alpha$ . To linear order in  $z_1$ , we find from Eq. (B5)

$$p_1 = -\frac{i\omega z_1}{i\omega + \alpha} \partial_x p_0 \quad (\text{B13})$$

The corresponding force is given by

$$f_1 \simeq \mathcal{A} z_1 \quad (\text{B14})$$

with

$$\mathcal{A} = i\omega\lambda + K + \chi, \quad (\text{B15})$$

where the active response  $\chi$  of the motors is given by

$$\chi = -N \int_0^l d\xi \frac{i\omega}{i\omega + \alpha} \partial_\xi p_0 \partial_\xi W_1 \quad (\text{B16})$$

For the choice of Eq. (B6) and (B8) the integral can be calculated and we obtain

$$\mathcal{A}(C, \omega) = i\omega\lambda + K - Nk_0 C \frac{i\omega/\alpha + (\omega/\alpha)^2}{1 + (\omega/\alpha)^2}. \quad (\text{B17})$$

Here, we have introduced the dimensionless control parameter  $C \equiv 2\pi^2\beta/\alpha$  with  $0 < C < \pi^2$  and the cross-bridge elasticity  $k_0 \equiv U/l^2$  of the motors.

## 3. Hopf bifurcation

A Hopf bifurcation occurs if there is a pair of values  $(C, \omega)$  for which  $\mathcal{A}$  as given by Eq. (B17) vanishes. Such a point indeed exists. For the critical value

$$C_c = \frac{\lambda\alpha + K}{Nk_0} \quad (\text{B18})$$

the bifurcation occurs for the critical frequency

$$\omega_c = \left( \frac{K\alpha}{\lambda} \right)^{1/2} \quad (\text{B19})$$

The critical frequency is bounded by the fact that  $C_c < \pi^2$ . The maximal frequency occurs for the maximal possible value of  $K$

$$K_{\max} = Nk_0\pi^2 - \lambda\alpha \quad (\text{B20})$$

for which  $C_c = \pi^2$ . This frequency is given by

$$\omega_{\max} = \alpha \left( N\pi^2 \frac{k_0}{\lambda\alpha} - 1 \right)^{1/2} \quad (\text{B21})$$

Note, that the maximal frequency can be significantly higher than the typical rate  $\alpha$  of the chemical cycle.

- 
- [1] Hudspeth, A.J. (1989) *Nature (London)* **341**, 397-404.
  - [2] de Vries, H.L. (1949) *Physica* **14**, 48-60.
  - [3] Gold, T. (1948) *Proc. Roy. Soc. B* **135**, 492-498.
  - [4] Hudspeth A.J. (1997) *Curr. Opin. Neurobiol.* **7**, 480-486.
  - [5] Dallos, P.J. (1992) *J. Neurosci.* **12**, 4575-4585.

- [6] Crawford, A.C. & Fettiplace, R. (1985) *J. Physiol.* **364**, 359-379.
- [7] Howard, J. & Hudspeth, A.J. (1988) *Neuron* **1**, 189-199.
- [8] Benser, M.E., Marquis, R.E. & Hudspeth, A.J. (1996) *J. Neurosci.* **15**, 5629-5643.
- [9] Zurek, P.M. (1981) *J. Acoust. Sci. Am.* **69**, 514-523.
- [10] Probst, R. (1990) in *New Aspects of Cochlear Mechanics and Inner Ear Pathophysiology* (ed. Pfaltz, C.R.) pp. 1-91 (Karger, Basel).
- [11] Strogatz, S.H. (1994) *Nonlinear Dynamics and Chaos* (Addison-Wesley, Reading, MA).
- [12] Choe, Y., Magnasco, M.O. & Hudspeth, A.J. (1998) *Proc. Natl. Acad. Sci. USA* **95**, 15321-15236.
- [13] Jaramillo, F., Markin, V.S. & Hudspeth, A.J. (1993) *Nature (London)* **364**, 527-529.
- [14] Cartwright, J.H.E., Gonzalez, D.L. & Piro, O. (1999) *Phys. Rev. Lett.* **82**, 5389-5392.
- [15] Jülicher, F. & Prost, J. (1997) *Phys. Rev. Lett.* **78**, 4510-4513.
- [16] Ruggero, M.A. (1992) *Curr. Opin. Neurobiol.* **2**, 449-456.
- [17] Ruggero, M.A., Rich, N.C., Recio, A., Narayan, S.S. & Robles, L. (1997) *J. Acoust. Soc. Am.* **101**, 2151-2163.
- [18] Couillet, P., Goldstein, R.E. & Gunaratne, G.H. (1989), *Phys. Rev. Lett.* **63**, 1954-1957.
- [19] Tilney, L.G. & Saunders, J.C. (1983) *J. Cell Biol.* **96**, 807-821.
- [20] Jacobs, R.A. & Hudspeth, A.J. (1990) *Cold Spring Harbor Symp. Quant. Biol.* **55**, 547-561.
- [21] Macartney, J.C., Comis, S.D. & Pickles, J.O. (1980) *Nature (London)* **288**, 491-492.
- [22] Manley, G.A. & Gallo, L. (1997) *J. Acoust. Soc. Am.* **102**, 1049-1055.
- [23] Jülicher, F., Ajdari, A. & Prost, J. (1997) *Rev. Mod. Phys.* **69**, 1269-1281.
- [24] Walczak, C.E. & Nelson, D.L. (1994) *Cell Motil. Cytoskeleton* **27**, 101-107.
- [25] Gibbons, I.R. (1981) *J. Cell Biol.* **91**, 107s-124s.
- [26] Kamimura, S. & Kamiya R. (1989) *Nature (London)* **340**, 476-478.
- [27] Camalet, S., Jülicher, F. & Prost, J. (1999) *Phys. Rev. Lett.* **82**, 1590-1593.
- [28] Howard, J. & Ashmore, J.F. (1986) *Hearing Research* **23**, 93-104.
- [29] Hudspeth, A.J. & Gillespie, P.G. (1994) *Neuron* **12**, 1-9.
- [30] Gillespie, P.G. & Corey, D.P. (1997) *Neuron* **19**, 955-958.
- [31] Denk, W., Webb, W.W. & Hudspeth, A.J. (1989) *Proc. Natl. Acad. Sci. USA* **86**, 5371-5375.
- [32] Hillery, C.M. & Narins, P.M. (1984) *Science* **225**, 1037-1039.
- [33] Koeppl, C.J. (1997) *Neurosci.* **17**, 3312-3321.
- [34] Holton, T. & Hudspeth, A.J. (1983) *Science* **222**, 508-510.
- [35] Scharf, B. (1983) in *Hearing Research and Theory, vol. 2* (eds. Tobias, J.V. & Schubert, E.D.), pp. 1-56 (Academic, NY).
- [36] Young, E. & Sachs, M.B. (1973) *J. Acoust. Soc. Am.* **54**, 1535-1543.
- [37] Wiesenfeld K. and Moss F. (1995), *Nature* **373**, 33-36.
- [38] Duke, T.A.J. & Bray, D. (1999) *Proc. Natl. Acad. Sci. USA* **96**, 10104-10108.
- [39] Delbrück, M. (1970) *Science* **168**, 1312-1315.